Karol Miller

School of Mechanical Engineering
The University of Western Australia
Crawley/Perth WA 6009, Australia
kmiller@mech.uwa.edu.au
http://www.mech.uwa.edu.au/kmiller/

Optimal Design and Modeling of Spatial Parallel Manipulators

Abstract

Parallel manipulators offer much higher rigidity and smaller mobile mass than their serial counterparts, thus allowing much faster and more precise manipulations. The main disadvantage of parallel robots is their small workspace in comparison to serial arms of similar size. Furthermore, the manipulability of parallel robots is often poor in some regions of the (already small) workspace. Another problematic issue is effective modeling of parallel robot dynamics, often needed for control algorithms. Dynamic algorithms developed for serial robots or general closed-loop mechanisms cannot be easily applied to parallel robots when the objective is real-time, dynamic-model-based control. Therefore, in this work we investigate how to design parallel manipulators so that their workspace size and manipulability are maximized, and how to model parallel robot dynamics effectively.

We develop a new performance index that combines measures of manipulability and workspace size, and a kinematic optimization process yielding a design that delivers the best compromise between manipulability and space utilization. Two examples are considered: the New University of Western Australia Robot (NUWAR) and the Linear Delta robot. Our experience in optimal design studies shows that the exhaustive search minimization algorithm is effective for as many as four independent design variables and presents a viable alternative to advanced non-linear programming methods.

We develop a method based on Hamilton's canonical equations to solve both the inverse and direct problems of dynamics for parallel robots. The method uses carefully chosen dependent coordinates, called here the coordinates of the extended space. The approach is shown to be computationally more efficient than the more common acceleration-based methods.

KEY WORDS—parallel robot, design, dynamics, manipulability, workspace

The International Journal of Robotics Research
Vol. 23, No. 2, February 2004, pp. 127-140,
DOI: 10.1177/0278364904041322

1. Introduction

The literature contains much information regarding various types of parallel robots (e.g., Merlet 2000; Tsai 1999). Parallel robots, unlike serial, traditional ones, have the end-effector connected to the base by several kinematic chains in parallel. Research into the field of parallel robots documented in the literature dates back to 1938, when Pollard (1942) patented his mechanism for car painting. In 1947 McGough proposed a six-degrees-of-freedom platform, which was later used by Stewart (1966) in his flight simulator. Parallel manipulators are particularly suited to a number of typical industrial applications and have been investigated by various researchers over the years. In recent years, several new structures and mechanisms have been proposed, developed for a variety of established and novel applications, such as packaging, assembly, haptic interfaces, etc. (Pierrot, Dauchez, and Fournier 1991; Badano et al. 1993; Herve 1994; Uchiyama 1994; Arai and Tanikawa 1996; Tsai 1997; Tsumaki et al. 1998). Most important here, however, is the development of the Delta, a three-degrees-of-freedom translational, spatial manipulator, by Clavel at the EPFL in Lausanne (Clavel 1988; Miller and Clavel 1992); see Figure 1.

Parallel manipulators possess a number of advantages when compared to traditional serial arms. Generally they offer much higher rigidity and smaller mobile mass than their serial counterparts. These features allow much faster and more precise manipulations. The main drawback of parallel manipulators is their small workspace, and often limited manipulability in certain regions of the workspace. Also, due to the presence of closed kinematic chains in the manipulator structure, the dynamics modeling, often necessary for control of high-speed manipulations, is not as straightforward as in the case of serial manipulators.

Problematic issues related to optimal design and dynamic modeling are amongst the most important research topics in the area of parallel manipulators. This contribution summarizes work on these topics conducted at the School of Mechanical Engineering, The University of Western Australia.

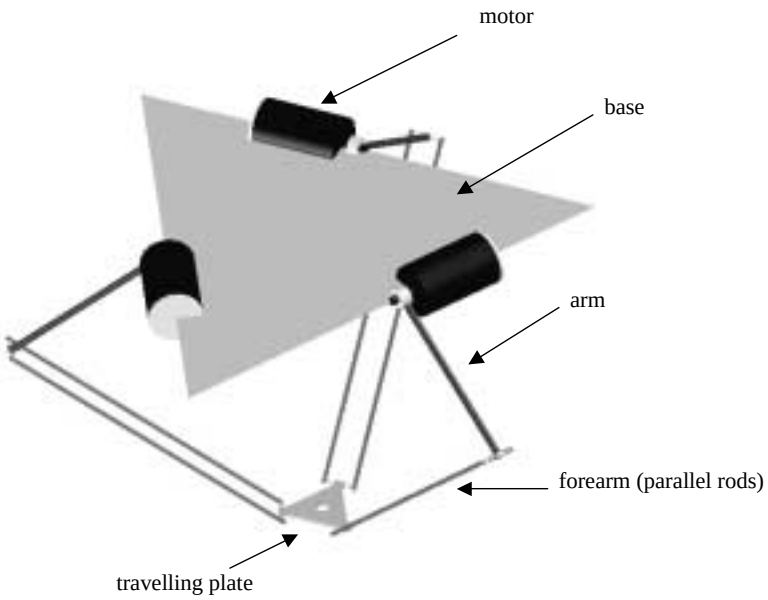

Fig. 1. Layout of Delta robot.

2. Optimal Design of Parallel Robots

2.1. Maximization of the Workspace Volume

After deciding on the kinematic structure of a manipulator (type design), often a designer is confronted by the task of maximizing the manipulator's workspace volume for a given size of a robot. In this section, an optimal design method is proposed suited for workspace maximization of spatial parallel manipulators.

Like the Delta (Figure 1), the robots considered here consist of three kinematic chains in parallel, which connect the base to the end-effector. For the given dimensions of a manipulator, it is of particular interest to determine how the size and shape of the robot workspace vary with values of two angles defining the orientation of the motor axes (Figure 2).

In addition to the dimensions of each component, two design variables (angles α and β) were introduced; α measures the inclination of each motor to the horizontal plane (for the Delta robot $\alpha = 0^\circ$) and β measures the rotation of each motor with respect to the vertical axis (for the Delta robot β=0°). As the arm is rigidly attached to its motor axis, the angles α and β control the orientation of the three-arm/forearm assemblies. Varying α and β angles leaves the locations of the three motors unchanged.

The choice of α and β resulting in maximum workspace volume was decided by an exhaustive search; the volume was calculated for $91 \times 91 = 8281$ combinations of design variable values from the interval $(0^\circ, 90^\circ)$. The details of the algorithm can be found in Miller (2002). The calculations show that the Delta configuration is not optimal in terms of the workspace volume. Other feasible configurations occur in the range $\alpha > 30^\circ$ and $\beta > 50^\circ$. The optimal motor axis orientation is given by $\alpha = 35.26^\circ$ and $\beta = 60^\circ$. It is worth noting that for such a choice of the design variables the motor axes are orthogonal. This configuration, known as the New University of Western Australia Robot (NUWAR), see Figure 2, has a workspace 9.4% larger than the workspace of the Delta, assuming that all dimensions are the same.

The results of the workspace volume maximization described in this section lead to the construction of the prototype; see Figure 2 (Miller 1998). NUWAR is one of the fastest robots in the world capable of achieving end-effector accelerations of 600 m s^{-2}.

2.2. Simultaneous Maximization of Workspace Volume and Manipulability[1]

When designing parallel manipulators it is often necessary to reach a compromise between two conflicting design goals: manipulability and workspace size. Maximization of the workspace volume alone tends to produce manipulators that are singular in all configurations, whilst considering manipulability in isolation may lead to architectures with relatively small workspaces; a clear example of this phenomenon may be found in the results of Stamper, Tsai, and Walsh (1997). Accordingly, the objective function considered in this section is a weighted sum of two performance indices, characterizing manipulability and workspace size.

1. This subsection is based on Stock (2000) and Stock and Miller (2003).

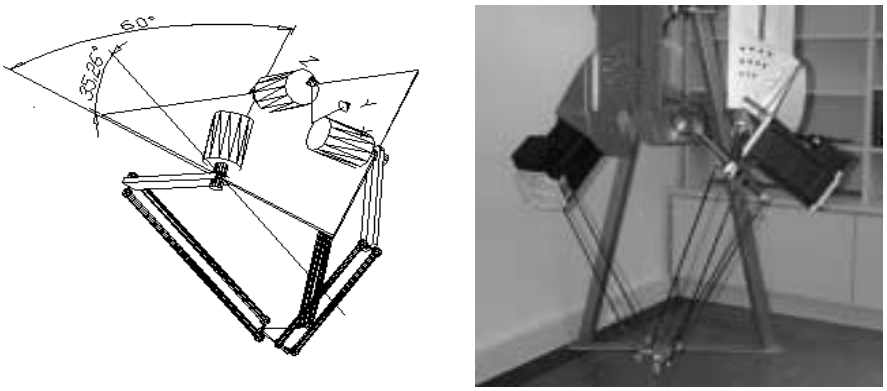

(a) (b)

Fig. 2. (a) Layout of NUWAR and (b) NUWAR prototype. The design variables are the inclination of each motor to the horizontal plane, α (= 35.26° for NUWAR and = 0° for Delta) and the rotation of each motor with respect to the vertical axis, β (=60° for NUWAR and =0° for Delta).

2.2.1. Performance Indices

Manipulability

The first performance index, η_1, measures the average value of the inverse of the condition number of the Jacobian matrix $1/\kappa_J$ over the workspace, normalized by the workspace volume, V_W:

$$\eta_1 = \frac{\int_{V_W} \frac{1}{\kappa_J} \mathrm{d}V_W}{\int_{V_W} \mathrm{d}V_W} = \frac{\int_{V_W} \frac{1}{\kappa_J} \mathrm{d}V_W}{V_W}. \tag{1}$$

Adapted from Gosselin and Angeles (1989), this index possesses several favorable characteristics. The index is normalized by the workspace size, and therefore gives a measure of kinematic performance independent of the differing workspace sizes of design candidates. Furthermore, the reciprocal of κ_J is bounded between 0 and 1, and is more convenient to handle than κ_J, which tends to infinity at singularities. Hence, during numerical integration, the number of sample points near singularities has a reduced effect on the result, since $1/\kappa_J$ approaches zero (rather than infinity) at these points. Finally, the (dimensionless) value of the index lies between zero, for a manipulator singular in all configurations, and unity, for a manipulator perfectly kinematically isotropic in all configurations.

Space Utilization

This performance index was developed in order to overcome the problems involved in applying simple performance indices in isolation. For example, attempts to optimize the structure by maximizing η_1 alone usually lead to architectures with a large structural space requirement but a workspace size tending to zero, whilst the maximization of the workspace volume often produces manipulators that are singular in all configurations. Clearly a practical optimization would require a utility function comprising multiple performance indices.

The space utilization performance index is defined as

$$\begin{aligned} \eta_2 &= \frac{\text{Workspace Volume}}{\text{Bounding Box Volume}} \\ &= \frac{V_W}{\text{Bounding Box Volume}} \end{aligned} \tag{2}$$

where the bounding box is defined as the smallest rectangular prism, whose sides are parallel to the global coordinate axes, containing all fixed actuators and every point within the workspace. The space utilization value reflects the ratio of workspace size to the physical size of the robot's structure. The index is dimensionless, bounded by the range [0 1], its calculation is simple and inexpensive (cf. numerical integration of the Jacobian condition number), and its value is independent of the overall scale of each design that it is applied to. Most importantly, designs requiring large volumes of space, but yielding small workspaces, are penalized. The utility function for maximization is therefore defined as

$$\begin{aligned} \eta &= w_1 \left(\frac{\int_{V_W} \frac{1}{\kappa_J} \mathrm{d}V_W}{V_W} \right) \\ &\quad + w_2 \left(\frac{V_W}{\text{Bounding Box Volume}} \right) \\ &= w_1 \eta_1 + w_2 \eta_2. \end{aligned} \tag{3}$$

The function is bounded by the range $[0 \quad (w_1 + w_2)]$, and is independent of both the overall scale of the design candidate

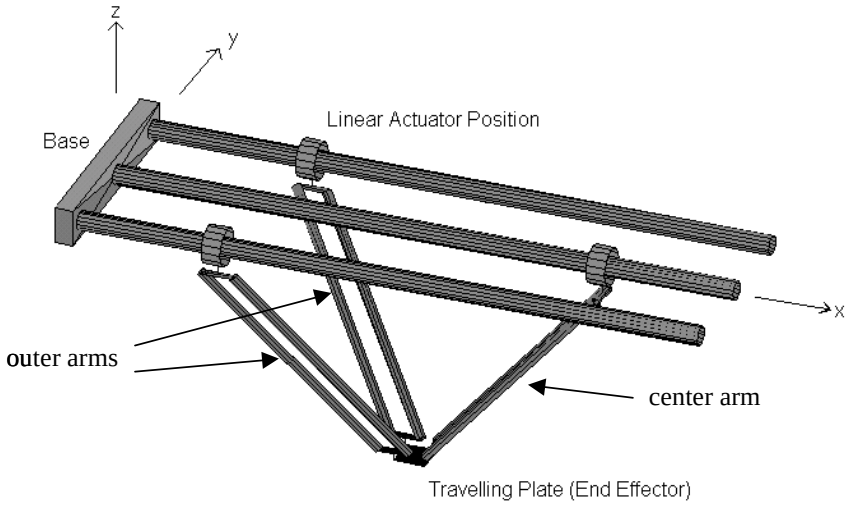

Fig. 3. Render MATLAB representation of the Linear Delta.

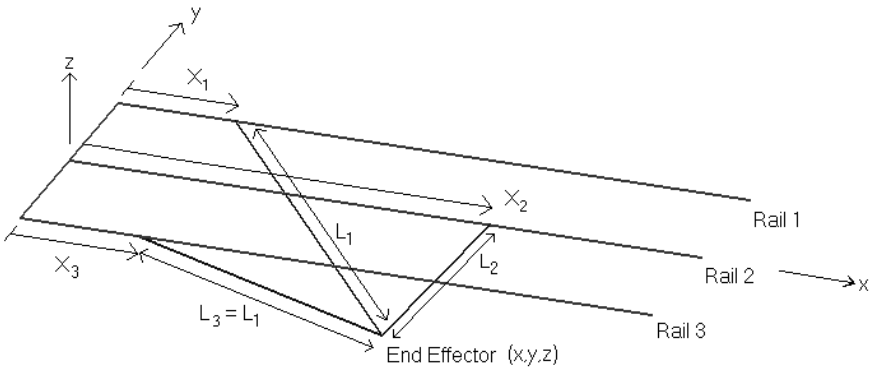

Fig. 4. Wireframe representation of the Linear Delta showing nomenclature.

to which it is applied and the limits chosen for the design variables (since neither performance index is normalized by its maximum observed value).

2.2.2. Application Example: Linear Delta Robot

The method was applied to the Linear Delta Robot (Figures 3, 4 and 5).

In order to reduce the number of variables and render the results independent of the scale of each design candidate, several non-dimensional ratios were chosen as the design variables. These variables, shown in Table 1, were selected to reflect intuitive measures of the relative proportions of the Linear Delta robot.

When considering regions away from the limits of travel of the actuators, the Linear Delta's workspace cross-section in the y–z plane, A_w, is constant, with its boundaries defined by the following.

Three circles, each centered on one actuator's position, with a radius equal to the length of the corresponding parallelogram arms (L_1 or L_2).

The plane $z = 0$, through which the end-effector cannot pass.

If $Z_R < 0$, the position of the central actuator restricts the inward motion of the outer arms.

In practice, the rails of the Linear Delta are long, and therefore it is reasonable to assume that, from the perspective of workspace calculations, the rails are infinite. This allows the ratio of the workspace volume to the bounding box volume to be replaced by the ratio of the *YZ* cross-sectional area of the workspace to the *YZ* cross-sectional area of the bounding box.

2.2.3. Computational Issues

An exhaustive (brute force) search method was used to solve the optimization problem. Whilst computationally expensive, an exhaustive search is simple, reduces the probability of any

Table 1. Kinematic Design Variables

Variable	Description	Restrictions
$\frac{L_1}{Y_R}$	Ratio of outer arm length to actuator separation	≥ 1
$\frac{Y_A}{Y_R}$	Ratio of center actuator horizontal eccentricity to actuator separation	0 – 1
$\frac{Z_R}{Y_R}$	Ratio of center actuator vertical eccentricity to actuator separation	
$\frac{L_2}{L_1}$	Ratio of center arm length to outer arm length	≥ 0

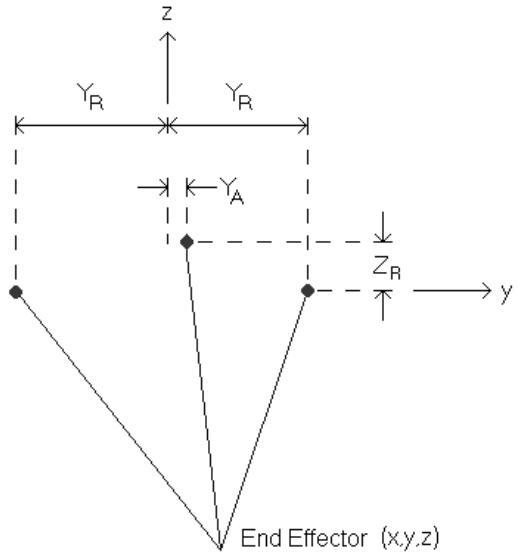

Fig. 5. End view (y–z plane) of wireframe representation showing nomenclature.

local maxima being overlooked, and provides information regarding the behavior of the utility function over the entire range of allowable values for each of the design variables.

The limits selected for the design variables were as follows: $1.4 \leq L_1/Y_R \leq 2.7$; $0 \leq Y_A/Y_R \leq 0.7$; $-0.5 \leq Z_R/Y_R \leq 0.5$; $0.6 \leq L_2/L_1 \leq 1.8$. Several of these limits are necessary to ensure that the resulting structure is practical. The remaining limits were chosen heuristically, with alterations made on a trial-and-error basis to yield a reasonably large range, and to ensure the inclusion of any local maxima of the utility function. A notable exception is the case where the manipulability index, η_1, was considered in isolation (i.e., $w_2 = 0$); in this situation L_2/L_1 was allowed to approach zero.

Since there is no analytical means of calculating the Jacobian condition number (κ_J), and therefore no closed-form expression for the manipulability index, numerical integration is required to determine the value of the utility function. The integral of eq. (1) may be approximated by a discrete sum

$$\eta_1 = \frac{\int_{A_W} \frac{1}{\kappa_J} \mathrm{d}A_W}{A_W} \approx \frac{\sum_{a \in A_W} \frac{1}{\kappa_J}}{N_a}, \tag{4}$$

where each a is one of N_a integration points in the y–z plane workspace cross-section. These points were generated by examining the boundaries of the cross-section and forming a uniformly distributed grid inside it.

In the majority of cases, closed-form methods may be utilized to calculate the exact cross-sectional area of the workspace (A_W). However, in some instances the choice of design variables precludes the application of the closed-form solutions, and it was necessary to approximate A_W. The following approximation was used

$$A_W \approx \mathrm{d}A_W N_a \tag{5}$$

where $\mathrm{d}A_W$ is the small area associated with each of the N_a integration points. The accuracy of the approximation in eq. (5) increases as N_a increases. Application of this equation to several situations in which a closed-form solution for A_W existed revealed that if $\mathrm{d}A_W$ was sufficiently small such that $N_a >$ 5000, then the relative error in A_W for these cases was generally less than 0.1%.

The complete four-dimensional optimization, programmed in MATLAB 5.3 (MATLAB 1999) required about three hours of computations using Pentium II 200 MHz PC.

2.2.4. Optimization Results

Since the weights of the utility function, w_1 and w_2 in eq. (3), are necessarily subjective, results for several combinations of values are presented in Table 2. The tendency for the solution to converge on zero workspace size architecture when manipulability was optimized alone was the reason for developing the second performance index, space utilization. Other behaviors of the manipulability index that were noted include the confirmation that the optimal value of Y_A is zero (a symmetrical architecture), and that for an arbitrary cross-section through the four-dimensional data set manipulability generally exhibits little variation when compared to space utilization.

Table 2. Optimization Results

Weights	Description	$\left(\frac{L_1}{Y_R}, \frac{Y_A}{Y_R}, \frac{Z_R}{Y_R}, \frac{L_2}{L_1}\right)$
$w_1 = 1$, $w_2 = 0$	Manipulability alone	(1.55, 0, –0.75, $\rightarrow$0)
$w_1 = 1$, $w_2 = 0$	Manipulability alone, with $Z_R = 0$	(1.48, 0, 0, 0.56)
$w_1 = 0$, $w_2 = 1$	Space utilization alone	(2.00, 0, 0, 0.60)
w_1 = 1, w_2 = 1	**Equally weighted utility function**	**(2.00, 0, 0, 0.63)**

Visualization via several surface plots greatly aids the interpretation of these results. Figure 6 shows the values of (a) $\eta = \eta_1 + \eta_2$, (b) η_1, and (c) η_2. In order to present the four-dimensional data set, two planes are displayed, each of which passes through the optimum point highlighted in Table 2.

The optimum architecture is relatively insensitive to increasing w_1; large increases in the weighting of manipulability ($w_1 > 3$) are necessary before a considerable change in geometry is noted. Whilst small increases in w_2 affect the results of the optimization, the change is limited to the variable L_2/L_1, with the greatest possible variation being a decrease of 0.03.

Currently, a Linear Delta prototype intended for cutting the shape of surfboards is under construction.

3. Parallel Robot Dynamics Using Hamilton's Equations in Extended Space

Fast and precise robot manipulation requires control algorithms that make the best use of the information extracted from the dynamic analysis of the robot: feedforward, computed torque (An et al. 1989); resolved acceleration (Luh, Walker, and Paul 1980), model-reference adaptive control (Liegois, Fournier, and Aldom 1980, and references therein). Common to all these control approaches, except the last, is the difficulty of solving the inverse dynamics problem for manipulators, and the challenge of doing so in real time. This has necessitated an adapted numerical representation and a high computing efficiency. The intrinsic nature of the NUWAR parallel robot (Miller 1998) is representative of most of the complexities and difficulties commonly encountered in the dynamic modeling of parallel structures. These include problematic issues such as the complicated, spatial kinematic structure, which includes many passive joints, the dominance of inertial forces over the frictional and gravitational components, and rapidly changing dynamics, which places restrictions on the length of the sampling interval and hence limits controller sophistication (i.e., the available inverse dynamics calculation time), etc.

3.1. Coordinate Choice for the Description of a Parallel Robot: Concept of the Extended Space

A number of approaches to the task of developing models of parallel robot dynamics have been proposed (e.g., Luh and Zheng 1985; Nakamura and Ghodoussi 1989; Lin and Song 1990; Miller and Clavel 1992; Zhang and Song 1993; Miller 1995; Baiges and Duffy 1996; Etemadi et al. 1997; Nenchev, Bhattacharya, and Uchiyama 1997; Wang and Gosselin 1998). These methods assume the manipulator to be a system of rigid bodies connected by ideal kinematic pairs without friction. Most often the closed kinematic chains are "temporarily cut" (artificially separated), and well-known efficient algorithms are utilized for the solution of the dynamics problem for the resulting tree structure. As the model is developed further, the cuts are removed by the introduction of closure conditions (holonomic constraints). This allows the results obtained for the tree structure to be transformed into those of the original closed-loop mechanism.

Such approaches fail in many cases with more complex spatial kinematic structures (such as that of the NUWAR), when the intended purpose of the development is that of real-time control. The reason for failure is a large number of passive degrees of freedom, which in the tree-structure approach require description; one differential equation of motion for each passive degree of freedom, often resulting in too large a number of equations for real-time applications. The computational complexity of such algorithms grows linearly with the number of relative coordinates (degrees of freedom) of the tree structure. NUWAR possesses 21 rotational joints, and the number of relative coordinates of its tree structure is 15. The number of independent coordinates is three.

When applying energy-based methods for non-redundant mechanisms, there is a strong temptation to select a minimal set of (independent) coordinates in joint space. Since NUWAR has three degrees of freedom, one is naturally inclined to select three generalized coordinates, e.g., angles in actuated joints ($\theta_i, i = 1, \ldots, 3$), and then to evaluate a set of three Lagrange equations of the second kind for these coordinates. Such equations would be the formulae for the unknown control torques. However, due to the complexity of the geometrical model, the evaluation of the Lagrangian (or Hamiltonian) and especially its derivatives (which would have to include also the derivatives of the solutions of equations of the model of geometry) with only three coordinates, is found to be extremely involved and tedious.

Another way of formulating equations of motion in independent coordinates is based on the concept of projection to the space tangent to constraints (Blajer 1992). The variation of

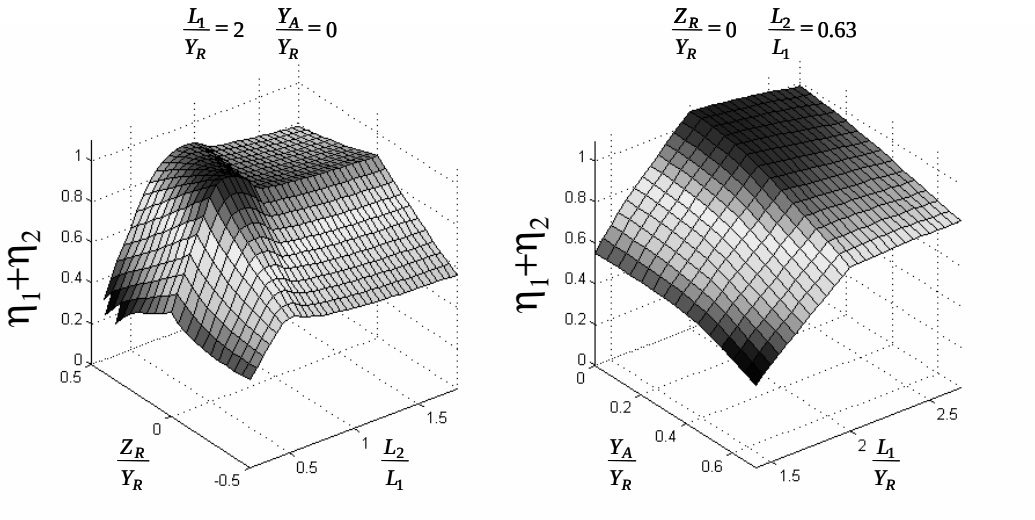

(a)

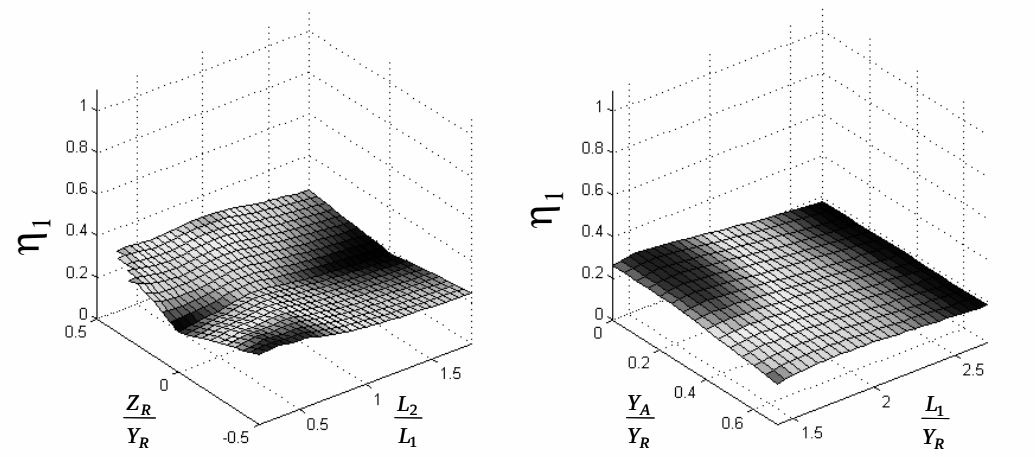

(b)

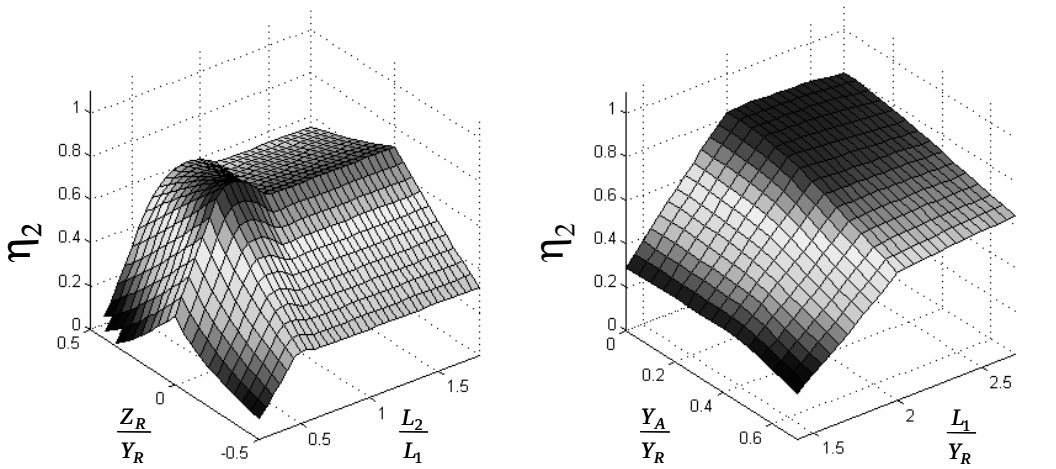

(c)

Fig. 6. Optimization results.

this method, leading to the formulation of the Kane equations has been recently applied in Tsai (2000) to a Gough–Stewart platform.

The formulation in dependent coordinates leads to more efficient algorithms. However, it would be expected that it is possible to devise better approaches than those using all dependent coordinates of the robot's tree structure (15 for NUWAR). My approach is to choose smartly such coordinates describing the manipulator that would be suitable for evaluation of the Lagrangian of the robot, and simultaneously their number would be smaller than the number of relative coordinates of the corresponding tree structure (equivalent single-degree-of-freedom joints). The modeling method presented in this section is not valid for general closed-loop mechanisms. However, it is effective for mechanisms that have a maximum of two links in each kinematic chain linking a base and an end-effector. To the best of my knowledge, there are no parallel robots described in the literature that would not satisfy this condition.

Of principal interest in the case of the non-redundant parallel robot analysis and control are the behaviors of the traveling plate and the actuated joints. Therefore, for the robot description, I propose the use of all coordinates belonging to the sum of the task and joint spaces of the robot. In the case of a three-degrees-of-freedom spatial manipulator they are

$$\{q_i\} = \{x, y, z, \theta_1, \theta_2, \theta_3\}, i = 1, \ldots, 6,$$

where $\{x, y, z\}$ describe the position of the center of the traveling plate, and $\{\theta_1, \theta_2, \theta_3\}$ denote the angles in the actuated joints. For such a set of coordinates $\{q_i\}$ I propose the name "extended space" (see also Miller and Clavel 1992; Guglielmetti 1994).

In the case of the three-degrees-of-freedom NUWAR robot, which possesses 21 rotational joints, the number of coordinates in the extended space is six, which is considerably fewer than the number of relative coordinates of NUWAR's tree structure.

Derivation of the Lagrange function for NUWAR in the extended space is relatively straightforward. Positions, velocities, and potential and kinetic energy of the arms are described using coordinates belonging to the joint space $\{\theta_1, \theta_2, \theta_3\}$. Position, velocity, and potential and kinetic energy of the traveling plate are described using coordinates belonging to the task space $\{x, y, z\}$. Positions and velocities of the top ends of forearms are described using coordinates belonging to the joint space $\{\theta_1, \theta_2, \theta_3\}$, and those of the bottom ends using coordinates belonging to the task space $\{x, y, z\}$. Knowing the positions and velocities of the ends of the forearms it is easy to derive equations for their kinetic and potential energies (Miller and Clavel 1992). The calculation of constraint derivatives (manipulator geometrical model equations, which relate controlled joint angles and the traveling plate position) is also simple. The constraint derivatives are of much simpler form than the derivatives of the solution of the inverse kinematics problem (inverse Jacobian) of the robot.

3.2. Application of Hamilton's Canonical Equations to Parallel Robot Dynamics Modeling

The method described in this section uses Hamilton's equations (for an introduction to Hamilton's method, see for example Lanczos 1962). The method is applicable to any multibody system constrained by geometric (holonomic) and/or velocity (non-holonomic) constraints. However, when considering dynamics of parallel robots we deal with scleronomous (not dependent explicitly on time) geometric constraints resulting from closed-chain architecture, so that to simplify derivations velocity (non-holonomic) and rheonomous (explicitly dependent on time) constraints are not considered below (for the derivation of the general case, see for example Gutowski 1971).

The method's effectiveness is amplified when the system under consideration is described by coordinates of the extended space.

Generalized momenta $\mathbf{p}$ can be presented in the following form

$$\mathbf{p} = \frac{\partial L}{\partial \dot{\mathbf{q}}} = \frac{\partial (\frac{1}{2}\dot{\mathbf{q}}^{\mathrm{T}} \cdot \mathbf{M} \cdot \dot{\mathbf{q}})}{\partial \dot{\mathbf{q}}} = \mathbf{M} \cdot \dot{\mathbf{q}} \tag{6}$$

where L is the Lagrangian, $\mathbf{q}$ is the vector of dependent coordinates and $\mathbf{M}$ is the mass matrix. Similarly

$$\begin{aligned} &\frac{\partial H}{\partial \mathbf{q}} = \frac{\partial (\mathbf{p}^{\mathrm{T}}\dot{\mathbf{q}} - L)}{\partial \mathbf{q}} = -\frac{\partial L}{\partial \mathbf{q}} = -L_{\mathbf{q}} \\ &\Rightarrow \; -L_{\mathbf{q}} = \mathbf{Q}_{ex} - \Phi_{\mathbf{q}}^{\mathbf{T}}\lambda - \dot{\mathbf{p}} \; \Rightarrow \\ &\Rightarrow \; \dot{\mathbf{p}} = L_{\mathbf{q}} + \mathbf{Q}_{ex} - \Phi_{\mathbf{q}}^{\mathbf{T}}\lambda \end{aligned} \tag{7}$$

where H is the Hamiltonian, $\mathbf{Q}_{ex}$ is the vector of external forces, $\mathbf{\Phi}_q$ is the Jacobian of the constraint equations and λ is the vector of unknown Lagrange multipliers.

Equations (6) and (7) form the following canonical equations:

$$\mathbf{p} = \mathbf{M} \cdot \dot{\mathbf{q}} \tag{8}$$

$$\dot{\mathbf{p}} = L_{\mathbf{q}} + \mathbf{Q}_{ex} - \Phi_{\mathbf{q}}^{\mathbf{T}} \cdot \lambda. \tag{9}$$

The formulation presented here is general enough to include any external forces, provided they act in (or can be projected onto) directions described by coordinates of extended space; these include actuator forces (directions belonging to the joint space) and forces acting on the end-effector (directions belonging to the task space). Other external forces (e.g., point forces acting on arms or forearms) cannot be included in the proposed formulation. In practice Delta-type parallel robots (e.g., NUWAR) are most often used as ultra-fast pick and place robots, so that it is reasonable to explicitly consider the case with zero external forces acting on the end-effector.

Equations (8) and (9) and the model of the robot's geometry were used to derive the equations of motion for NUWAR. $\mathbf{M}$, L_q and $\mathbf{\Phi}_q$ were evaluated using Mathematica (Wolfram 1999), using similar a method to that described in Miller and Clavel (1992) for the Delta robot.

The final forms of the equations governing the motion of NUWAR are

$$\mathbf{p} = \mathbf{M}.\dot{\mathbf{q}}, \mathbf{q} = \{x, y, z, \theta_1, \theta_2, \theta_3\} \tag{10}$$

$$\dot{\mathbf{p}}_t = L_\mathbf{q} - \Phi_\mathbf{q}^\mathbf{T} \cdot \lambda, \tag{11}$$

in the directions belonging to the task space $\{x, y, z\}$,

$$\dot{\mathbf{p}}_j = L_\mathbf{q} + \mathbf{Q}_{ex} - \Phi_\mathbf{q}^\mathbf{T} \cdot \lambda, \tag{12}$$

in the directions belonging to the joint space $\{\theta_1, \theta_2, \theta_3\}$,

$$\Phi_i = 0, \quad i = 1, \ldots, 3. \tag{13}$$

where $\mathbf{p}_t$ and $\mathbf{p}_j$ denote generalized momenta in the directions belonging to task and joint spaces, respectively: $\mathbf{p} = \{\mathbf{p}_t, \mathbf{p}_j\}$. There are no $\mathbf{Q}_{ex}$ terms in the first three equations for $\dot{\mathbf{p}}_t$ (eq. (11)) because these equations correspond to the x, y and z coordinates. The only external forces acting on NUWAR are torques corresponding to the θ_1, θ_2, and θ_3 coordinates (eq. (12)).

3.3. Solution of the Inverse Problem of Dynamics

In the case of the inverse problem of dynamics, i.e., trajectory known, external forces (desired motor torques) unknown, three steps are required to arrive at the solution of eqs. (10)–(12).

1. In the first step, the generalized momenta are evaluated in directions $x, y, z, \theta_1, \theta_2, \theta_3$ from eqs. (10) for the time instant t. Only generalized positions and velocities are required as input. Accelerations are not needed. For the trajectory start point with the initial conditions of zero velocities, these terms can safely be initiated to zero.

2. In the second step, it is possible to substitute the numerically calculated derivatives of momenta (using, for example, a two-point formula) $\dot{p}_x$, $\dot{p}_y$, $\dot{p}_z$ into eq. (11) for the directions x, y, z belonging to the task space of the robot. These three equations for any given position (on the desired trajectory) constitute a set of three linear equations from which the required multipliers λ_j, $j =$ 1,2,3 can be easily obtained.

3. After the substitution of the derivatives of generalized momenta in directions θ_1, θ_2, θ_3 belonging to the joint space of the robot, and the multipliers λ_1, λ_2, λ_3, eqs. (12) become the explicit formulae for torques Q_{exi}, $i =$ 4,5,6.

Often the trajectory of very fast parallel robots (e.g., NUWAR) is commanded as a sequence of points with a sampling period of 1 ms or lower. Velocities and accelerations are calculated numerically. This allows for the flexibility of not knowing the trajectory beforehand. An important feature of the model obtained by the Hamilton-based approach is that the solution of the inverse problem does not require acceleration information (measurements or estimates) as an input state to the model. Only the positions x, y, z, θ_1, θ_2, θ_3 and the corresponding velocities are necessary. Instead of accelerations it is necessary to provide derivatives of momenta obtained numerically. This approach removes usually long terms of the form $\frac{\mathrm{d}}{\mathrm{d}t}(\frac{\partial L}{\partial \dot{q}})$ from the equations and simplifies calculations. This advantage can save time in the calculation of kinematics and simultaneously improve model accuracy. The presence of accelerations in dynamic models obtained by Newton–Euler and Lagrange based approaches is inherent. The application of Hamilton's canonical equations eliminates this requirement.

In the case of commanding exact values of acceleration, the formulation presented here has no advantage as far as accuracy of the solution of the inverse problem is concerned (no disadvantage either if the sampling period is small enough, as it indeed is in practice), but the computational efficiency advantage remains.

The Hamilton-based method was compared to the Lagrange formulation (Miller and Clavel 1992). Both formulations use the coordinates of the extended space. Calculations showed that the inverse dynamics model based on the method of Hamilton required 28% fewer floating-point operations than the more traditional Lagrange based one, due to not having to evaluate lengthy terms of $\frac{\mathrm{d}}{\mathrm{d}t}(\frac{\partial L}{\partial \dot{q}})$. Computational results obtained using both methods were almost identical (within 0.01 N).

3.4. Solution of the Forward Problem of Dynamics

In the case of the forward problem of dynamics, the dynamical equations (10)–(12) and constraint equations (13) form a system of differential-algebraic equations (DAEs). Usually, solving DAEs is considerably more difficult than integrating systems of ordinary differential equations (ODEs). See, for example, Bayo and Garcia de Jalon (1994) and Blajer (1998) and references therein; the second reference is particularly worth recommending because it contains a large bibliography of Russian language multibody systems literature. Even though a number of multibody systems researchers suggest that obtaining solutions to DAEs can cause serious trouble, I obtained accurate simulation results using a straightforward method, based on transforming DAEs into the system of ODEs by differentiating (once) equations of geometrical constraints and using a standard fourth/fifth-order stepping procedure (ODE45 in MATLAB 1999) with Baumgarte stabilization (Baumgarte 1972).

The solution algorithm used in this work was proposed by Lankarani and Nikravesh (1988). In order to avoid mixed differential and algebraic equations the Lagrangian needed to be modified to include the kinematic velocity constraints.

$$L^* = L + \dot{\Phi}^{\mathbf{T}}\sigma \tag{14}$$

where σ is a new set of Lagrange multipliers. It is easy to demonstrate that the Lagrange multipliers λ used in eqs. (7), (8), (11), and (12) are simply the time derivatives of the introduced multipliers σ. The resulting modified Hamiltonian is

$$H^* = \mathbf{p}^{\mathbf{T}}\dot{\mathbf{q}} - L^*. \tag{15}$$

Substitution to eqs. (8) and (9) gives

$$\mathbf{p} = \mathbf{M}\dot{\mathbf{q}} - \Phi_{\mathbf{q}}^{\mathbf{T}}\sigma \tag{16}$$

and

$$\dot{\mathbf{p}} = L_{\mathbf{q}} + \mathbf{Q}_{ex} - \dot{\Phi}_{\mathbf{q}}^{\mathbf{T}}\sigma. \tag{17}$$

The above set of differential equations needs to be supplemented by equations of kinematic constraints:

$$\dot{\Phi} = \Phi_{\mathbf{q}}\dot{\mathbf{q}} = 0. \tag{18}$$

Equations (16)–(18) constitute a system of $2n + m$ (where n is the number of dependent coordinates, m is the number of constraints, $n - m$ = number of degrees of freedom; for NUWAR, described by coordinates of the extended space, $n = 6$, $m = 3$) ODEs, with $\mathbf{p}$, $\mathbf{q}$ and σ as unknowns.

Only $n + m$ equations must be solved at each time step in the numerical implementation of the algorithm. The following three steps are required to arrive at the solution of the forward problem of dynamics.

1. Equations (16) and (18) are solved for $\dot{\mathbf{q}}$ and σ at time t (when the values of $\mathbf{p}$ and $\mathbf{q}$ are known; initial condition):

$$\begin{bmatrix} \mathbf{M} & \Phi_{\mathbf{q}}^{\mathbf{T}} \\ \Phi_{\mathbf{q}} & \mathbf{0} \end{bmatrix} \begin{Bmatrix} \dot{\mathbf{q}} \\ -\sigma \end{Bmatrix} = \begin{Bmatrix} \mathbf{p} \\ \mathbf{0} \end{Bmatrix}. \tag{19}$$

2. Formula (17) is used to compute $\dot{\mathbf{p}}$ explicitly. No solution of equations is required here.

3. Vectors $\mathbf{p}$ and $\mathbf{q}$ at time $(t + \Delta t)$ are obtained by numerical integration. Upon convergence, the time variable is updated and the next step initiated.

The method was verified by feeding the solution for time histories of control torques obtained from the inverse dynamics algorithm into the forward dynamics algorithm. The trajectory initially used as the input to the inverse dynamics algorithm was reproduced almost exactly. This validates the appropriateness and accuracy of methods used. As the Hamilton-based inverse dynamics algorithm gave almost identical results to the Lagrange-based one, and the Hamilton-based forward dynamics algorithm produced expected results, the presence of a symmetrical error in both inverse and forward dynamics algorithm implementation is highly unlikely. The results of computer simulations are presented in Section 3.5.

It should be noted here that the formulation of equations of motion based on Hamilton's equations possesses an inherent advantage over acceleration-based formulations. The system of Hamilton's equations with multipliers is of index two; acceleration based formulations result in systems of DAEs of index three; for discussion, see Blajer (1998) and Brenan, Campbell, and Petzold (1989). The Hamilton-based algorithm was compared to the acceleration-based (Lagrange in extended space) formulation. An identical ODE integration method with Baumgarte stabilization was used, see Frame (1999). This confirmed the observation of Lankarani and Nikravesh (1988) that, since only one time derivative of the constraints is used (eq. (18)), the integration of eqs. (16)–(18) is more efficient and stable than the integration of equations resulting from acceleration-based formulations. When using acceleration-based formulations, the geometric constraints have to be differentiated twice to avoid the integration of the mixed differential-algebraic system. This leads to larger constraint violations.

3.5. Results of Computer Simulations

Computer simulations were performed for the prototype of NUWAR (Miller 1998):

- length, mass and moment of inertia of the arm are 0.26 m, 0.977 kg, and 0.01822 kg m^2;
- length and mass of the forearm are 0.48 m and 0.0296 kg;
- radial distance of each motor from the centerline is 0.194 m;
- displacement in the radial direction of the mid-point of each pair of spherical joints on the traveling plate is 0.03 m;
- spacing of the forearms is 0.05 m;
- traveling plate mass is 0.2807 kg;
- parallelogram-control arm joint mass is 0.0099 kg.

A vast range of trajectory types was generated. The geometric shapes included straight line, ellipse, sheared ellipse, and clothoid. The time–motion programs used were parabolic ("bang-bang"), cycloidal ("sine on ramp") and fifth-order polynomial (LePage 1999). The trajectories served as input

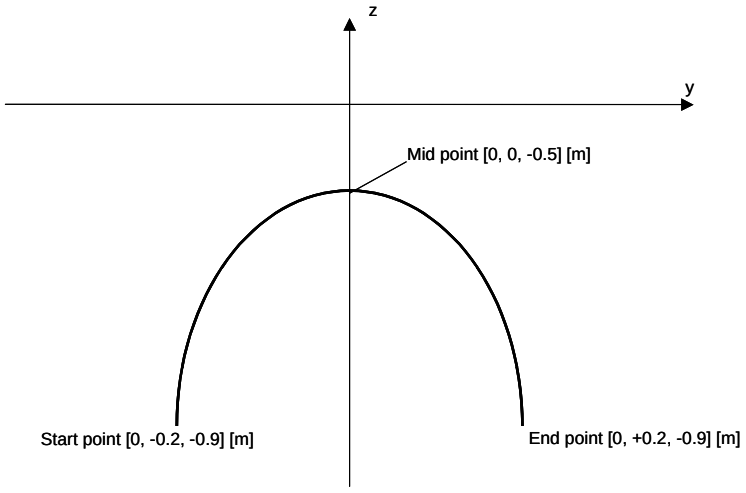

Fig. 7. Elliptical trajectory used as input for simulations.

to inverse kinematics and inverse dynamics problems. Calculated motor torque time histories were used as input to forward dynamics calculations. Equation derivation was performed with Mathematica (Wolfram 1999). Numerical calculations and animation of results were performed with MATLAB (1999).

Here I present results for a typical, symmetrical, elliptical pick-and-place trajectory (Figure 7):

> start point -> [0, –0.2, –0.9] (m), corresponding to joint angles $\theta_1 = 70.95°$, $\theta_2 = 87.13°$, $\theta_3 = 51.65°$;
>
> mid-point -> [0, 0, –0.5] (m);
>
> end point -> [0, +0.2, –0.9] (m);
>
> time to traverse the ellipse -> 0.5 (s);
>
> and back to the start point, followed by the traveling plate according to the "3–4–5 polynomial" motion program. This results in continuous accelerations and finite jerks. The maximum accelerations of the traveling plate were 294.82 m s^{-2}.

Figure 8 shows time histories of motor torques required to execute the trajectory; the solution of the inverse dynamics problem. The maximum torques required are 33.14 Nm, which is close to the maximum torque from NUWAR's motors (41.76 Nm), so that the trajectory under discussion is close to the limit of the capabilities of the robot. It is worth noting that the maximum motor torques required by NUWAR are slightly less than those required by the Delta to follow the same trajectory (36.30 Nm).

Figure 9 presents the comparison of the trajectory calculated with a forward dynamics algorithm described in Section 3.4, using the motor torque histories of Figure 7, with the original trajectory used as the input to the inverse dynamics.

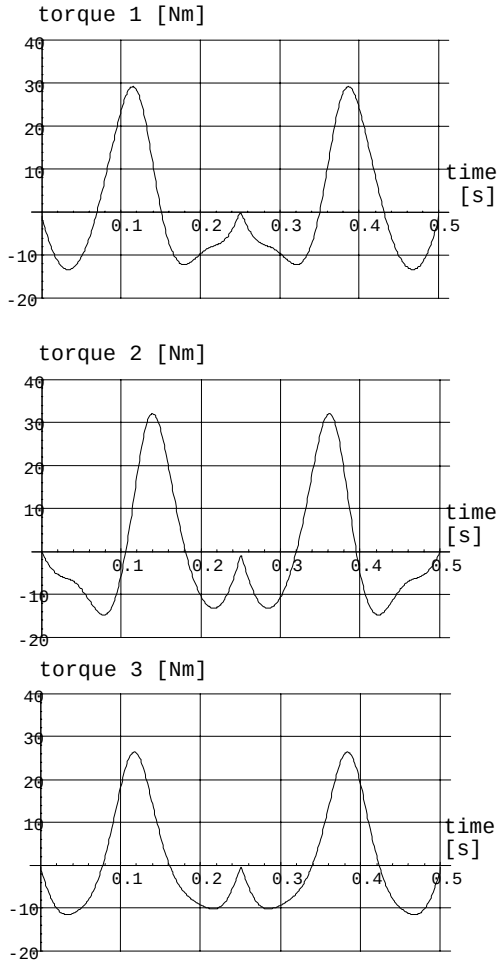

Fig. 8. Results of inverse dynamics calculations: time histories of motor torques required to produce the elliptical trajectory described above.

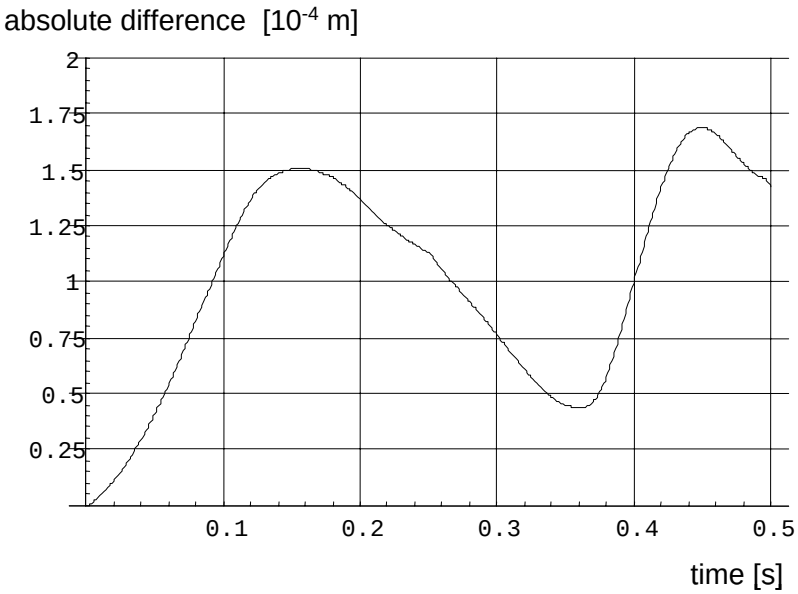

Fig. 9. Results of forward dynamics calculations: the difference between the trajectory serving as input to inverse dynamics and the result of forward dynamics calculations using torque histories of Figure 8.

The two trajectories match (almost) exactly proving the appropriateness and accuracy of methods proposed in this paper.

4. Conclusions and Discussion

A method of multidimensional kinematic optimization of the parallel robot's geometry was developed. For some architectures, like that of the NUWAR, the maximization of workspace volume alone gives satisfactory results. However, the maximization of the workspace volume without considering other issues often produces manipulators with very poor manipulability. To overcome this difficulty a utility function incorporating two performance indices was formulated in order to determine those architectures that yield an optimum compromise between manipulability and a new performance index, space utilization. Space utilization is a concept designed to overcome the problems of small, non-singular workspaces often encountered when a parallel manipulator is optimized with only manipulability in mind. The exhaustive search algorithm was used to reliably find all prospective design candidates in parameter space. The method was shown to work well for as many as four design variables and, therefore, is a viable competitor to advanced non-linear programming methods.

"Optimum" configuration could have different meanings in different contexts; e.g., in some applications a large workspace without necessarily high manipulability might be desired, in other cases manipulability needs to be emphasized. This can be achieved by a suitable choice of weighting factors in the cost function (3). The results presented here, and the suite of MATLAB programs created to perform the optimization, form a framework, which may be utilized to create and analyze designs that result from selecting weighting factors that are appropriate to a specific application.

An efficient method of solving dynamics of parallel robots was developed and applied to the NUWAR. The method was based on Hamilton's canonical equations in the extended space defined as a union of task and joint spaces of a robot. The use of coordinates of the extended space results in much fewer equations than in the case of using relative coordinates, and in a simple Lagrangian.

The use of Hamilton's equations is advantageous in application to the inverse problem of dynamics. This method is numerically more efficient than the more traditional Lagrange and Newton–Euler methods because Hamilton's equations do not require accelerations as input data to the inverse dynamics algorithm, and terms of the form $\frac{\mathrm{d}}{\mathrm{d}t}(\frac{\partial L}{\partial \dot{q}})$ involving accelerations are absent. This results in better accuracy of the algorithm.

The solution of the forward problem of dynamics was obtained without any difficulties by transforming the original system of DAEs to ODEs, and using a standard stepping algorithm with Baumgardte stabilization. The inherent advantage of using Hamilton's equations for the direct problem of dynamics is that, together with algebraic equations of constraints, they form the system of DAEs of index 2, not of

index 3 as is the case in the acceleration-based formulations. Numerical integration of index 2 systems is known to be more stable than solution of index 3 systems.

Acknowledgments

I would like to acknowledge the following students for their contributions to this work: on the NUWAR project, Shane Parker, Josh Male, Lachlan Roberts, Stephen LePage, Frances Garland, Nadine Frame, and Ben Hawkey; on the Linear Delta project, Michael Stock, Robert Davis, Matthew Fleming, and Dane Howarth. I would like to thank Dr Angus Tavner for carefully reading the manuscript. This work was funded by the Faculty of Mathematical and Engineering Sciences of The University of Western Australia and The Australian Research Council.

References

An, C. H., Atkeson, C. G., Griffiths, J. M., and Hollerbach, J. M. 1989. Experimental evaluation of feedforward and computed torque control. *IEEE Transactions on Robotics and Automation* 5(3):368–373.

Arai, T., and Tanikawa, T. 1996. Development of a new parallel manipulator with fixed linear actuator. In *Proceedings of Japan/USA Symposium on Flexible Automation*, Vol. 1, ASME, New York, pp.145–149.

Badano, F., Betempts, M., Burckhardt, C. W., Clavel, R., and Jutard, A. 1993. Assembly of chamferless parts using a fast robot. In *Proceedings of the 24th International Symposium on Industrial Robots*, Tokyo, Japan, pp. 89–96.

Baiges, I. J., and Duffy, J. 1996. Dynamic modeling of parallel manipulators. In *Proceedings of the 1996 ASME Design Engineering Technical Conference*, Paper No. 96-DETC/MECH-1136.

Baumgarte, J. 1972. Stabilization of constraints and integrals of motion in dynamical systems. *Computer Methods in Applied Mechanics and Engineering* 1:1–16.

Bayo, E., and Garcia de Jalon, J. 1994. *Kinematic and Dynamic Simulation of Multibody Systems: The Real-Time Challenge*, Springer-Verlag, New York.

Blajer, W. 1992. A projection method approach to constrained system analysis. *ASME Journal of Applied Mechanics* 59(3):643–649.

Blajer, W. 1998. *Methods of Multibody System Dynamics*, Technical University of Radom Publishers, Radom, Poland.

Brenan, K. E., Campbell, S. L., and Petzold, L. R. 1989. *The Numerical Solution of Initial Value Problems in Differential-Algebraic Equations*, Elsevier Science, Amsterdam.

Clavel, R. 1988. Delta, a fast robot with parallel geometry. In *Proceedings of the 18th International Symposium on Industrial Robots*, Lausanne, Switzerland, pp. 91–100.

Etemadi, K., Zanganeh, K., Sinatra, R., and Angeles, J. 1997. Kinematics and dynamics of a six-degrees-of-freedom parallel manipulator with revolute legs. *Robotica* 15:385–394.

Frame, N. 1999. *The Lagrange-based model of NUWAR dynamics*. BEng. Honours Thesis, Department of Mechanical and Materials Engineering, The University of Western Australia, Crawley/Perth.

Gosselin, C., and Angeles, J. 1989. The optimum kinematic design of a spherical three-degrees-of-freedom parallel manipulator. *ASME Journal of Mechanisms, Transmissions and Automation in Design* 111(2):202–207.

Guglielmetti, P. 1994. *Model-based control of fast parallel robots: a global approach in operational space.* PhD Thesis No. 1228, Swiss Federal Institute of Technology, Lausanne.

Gutowski, R. 1971. *Analytical Mechanics*, PWN, Warsaw, Poland.

Herve, J. M. 1994. Methodological design of new parallel robots via the Lie group of displacements. In *Proceedings of CISM/IFToMM Conference Ro.Man.Sy. '94*, Gdansk, Poland, pp. 301–306.

Lanczos, C. 1962. *The Variational Principles of Mechanics*, University of Toronto Press, Toronto.

Lankarani, H. M., and Nikravesh, P. E. 1988. Application of the canonical equations of motion in problems of constrained multibody systems with intermittent motion. In *Advances in Design Automation*, S. S. Rao, editor, ASME, New York, Vol. 14, pp. 417–423.

LePage, S. 1999. *Trajectory generation.* BEng. Honours Thesis, Department of Mechanical and Materials Engineering, The University of Western Australia, Crawley/Perth.

Liegois, A., Fournier, A., and Aldom, M. 1980. Model reference control of high-velocity industrial robots. In *Proceedings of Joint Automatic Control Conference*, San Francisco, CA.

Lin, Y. J. and Song, S. M. 1990. A comparative study of inverse dynamics of manipulators with closed-chain geometry. *Journal of Robotic Systems* 7:507–534.

Luh, J. Y. S. and Zheng, Y. F. 1985. Computation of input generalized forces for robots with closed kinematic chain mechanisms. *IEEE Journal of Robotics and Automation* 1:95–103.

Luh, M., Walker, M. W., and Paul, R. C. 1980. Resolved acceleration control of mechanical manipulators. *IEEE Transactions on Robotics and Automation* 25(3):468–474.

MATLAB. 1999. Version 5.3, Student Edition, Prentice Hall, Englewood Cliffs, NJ.

Merlet, J. P. 2000. *Parallel Robots*, Kluwer Academic, Dordrecht.

Miller, K. 1995. Experimental verification of modeling of Delta robot dynamics by direct application of Hamilton's principle. In *IEEE Conference on Robotics and Automation*, Nagoya, Japan, pp. 532–537.

Miller, K. 1998. Parallel robot. Australian Provisional Patent Application No. PP7518.

Miller, K. 2002. Maximization of workspace volume of 3-dof spatial parallel manipulators. *Transactions of the ASME, Journal of Mechanical Design* 124(2):347–350.

Miller, K., and Clavel, R. 1992. The Lagrange-based model of Delta-4 robot dynamics. *Robotersysteme* 8, Springer-Verlag, Berlin, pp. 49–54.

Nakamura, Y., and Ghodoussi, M. 1989. Dynamics computation of closed-link robot mechanisms with non-redundant and redundant actuators. *IEEE Transactions on Robotics and Automation* 5(3):294–302.

Nenchev, D. N., Bhattacharya, S., and Uchiyama, M. 1997. Dynamic analysis of parallel manipulator under the singularity-consistent parametrization. *Robotica* 15(4):375–384.

Pierrot, F., Dauchez, P., and Fournier, A. 1991. Hexa, a fast 6-degree-of-freedom fully parallel robot. In *Proceedings of the International Conference on Advanced Robotics*, Pisa, Italy, Vol. 2/2, pp.1158–1163.

Pollard, W. L. V. 1942. Position controlling apparatus, US Patent No. 2,286,571.

Stamper, R. E., Tsai, L.-W., and Walsh, G. C. 1997. Optimization of a three DOF translational platform for well-conditioned workspace. In *Proceedings of the 1997 IEEE International Conference on Robotics and Automation*, IEEE, Piscataway, NJ, Vol. 4, pp. 3250–3255.

Stewart, D. 1966. A platform with six degrees of freedom. *Proceedings of the Institution of Mechanical Engineers, Part I*, 180(15):371–386.

Stock, M. 2000. *The Linear Delta robot*. BEng. Honours Thesis, Department of Mechanical and Materials Engineering, The University of Western Australia, Crawley/Perth.

Stock, M., and Miller, K. 2003. Optimal kinematic design of spatial parallel manipulators; application to Linear Delta robot. *ASME Journal of Mechanical Design* 125(2):292–301.

Tsai, L. W. 1997. Multi-degree-of-freedom mechanisms for machine tools and the like, US Patent No. 5,656,905.

Tsai, L. W. 1999. *Robot Analysis: The Mechanics of Serial and Parallel Manipulators*, Wiley, New York.

Tsai, L. W. 2000. Solving the inverse dynamics of Stewart–Gough manipulator by the principle of virtual work. *ASME Journal of Mechanical Design* 122:3–9.

Tsumaki, Y., Narusew, H., Nenchev, D. N., and Uchiyama, M. 1998. Design of compact 6-dof interface. In *Proceedings of 1998 IEEE Conference on Robotics and Automation*, pp. 2581–2585.

Uchiyama, M. 1994. A 6 d.o.f. parallel robot HEXA. *Advanced Robotics* 8(6):601.

Wang, J., and Gosselin, C. M. 1998. A new approach for the dynamic analysis of parallel manipulators. *Multibody System Dynamics* 2:317–334.

Wolfram, S. 1999. *The Mathematica Book*, Cambridge University Press, Cambridge.

Zhang, C. D., and Song, S. M. 1993. An efficient method for inverse dynamics of manipulators based on virtual work principle. *Journal of Robotic Systems* 10(5):605–627.